phys. stat. sol. (b) **233**, No. 1, 31–38 (2002)

Fundamental Limits of Soft Magnetic Particle Composites for High Frequency Applications

R. RAMPRASAD[1]) (a), P. ZURCHER (a), M. PETRAS (a), M. MILLER (a), and P. RENAUD (b)

(a) Semiconductor Products Sector, Motorola, Inc., 2100 E. Elliot Road, Tempe, AZ, USA

(b) Semiconductor Products Sector, Motorola, Inc., 31023 Toulouse Cedex, Toulouse, France

(Received March 15, 2002; accepted May 25, 2002)

PACS: 75.50.Tt; 76.50.+g

A phenomenological model of magnetic nanoparticle composites consisting of ideal lossless particles with identical properties embedded in a non-magnetic matrix has been developed. The input material parameter for this model include the saturation magnetization (M_s) and the crystal anisotropy field (H_k) of the particles. The relationships between key magnetic properties like the low frequency effective permeability and the FMR frequency, and the material and physical attributes (such as shape, volume fraction, and packing type) of the particles have been identified using an iterative extension of the Bruggeman effective medium theory.

1. Introduction

The integration of on-chip inductors and transformers with magnetic materials of high permeability offers the potential benefits of a reduction in device size and an increase in performance – essential attributes for current high frequency technologies to remain competitive [1–4]. However, accomplishing these attributes without introducing significant losses, especially at GHz frequencies, appears to be a challenge. For instance, the ferromagnetic resonance (FMR) frequency, close to which a drastic degradation in permeability is observed, typically occurs at GHz (or even lower) frequencies in most high permeability materials. Thus, in addition to a large low frequency permeability, a large FMR frequency is also desired.

Promising soft magnetic materials for high frequency applications are nanostructured materials sputter deposited as thin films [5–9] and magnetic nanoparticle composites [10–13], the latter being the focus of the present study. The composite material is assumed here to consist of identical ideal ellipsoidal or cylindrical metallic ferromagnetic nanoparticles embedded in a non-magnetic matrix.

The FMR behavior of an individual particle is mainly determined by its shape and its intrinsic material properties [14, 15]. The present work establishes a connection between the intrinsic material properties of individual particles of given shape and the composite magnetic properties by generalizing the Bruggeman effective medium theory (EMT) [16–18] via an iterative scheme (which is necessary when the composite consists of non-spherical particles). It will be shown that the shape of the particles, along with their volume fraction and packing geometry, crucially determines tradeoffs between the

[1]) Corresponding author; e-mail: R.Ramprasad@motorola.com

 0370-1972/02/23309-0031 $ 17.50+.50/0

low frequency effective permeability of the composite and its FMR frequency. An additional degradation of the permeability could be caused by eddy current and magnetic damping losses of the particles, and dielectric losses of the non-magnetic matrix. These losses have not been included in the present model but will be explicitly considered elsewhere [19].

The composite model presented here requires the following material properties of the magnetic particles as input: The saturation magnetization, M_s, and the crystal anisotropy field, H_k. The saturation magnetization is the maximum attainable magnetization (at 0 K) per unit volume and is related to the number of electrons with unpaired spin in the material. The crystal anisotropy field is a measure of the extent to which magnetization in the bulk is preferred along one direction (the "easy" axis) versus others (the "hard" axes). The particles are assumed to have reached the saturation magnetization along the easy axis; under this assumption, the rotational permeability is maximal along the hard axes and unity along the easy axis [14, 15][2]). It is further assumed that the directions of the hard axes are orthogonal to the easy axis[3]).

It is worth mentioning that the magnetic permeability is, in general, a tensor. Unless otherwise stated, "permeability" in the present work refers to the diagonal components of the low frequency relative rotational permeability tensor along the direction of an appropriate hard axis[4]). Furthermore, we distinguish between three different permeabilities: Those of the bulk (μ^{bulk}), the particle (μ^{p}), and the composite (μ^{eff}). While μ^{bulk} is determined by M_s and H_k, μ^{p} is determined by M_s, H_k, and the particle shape, and μ^{eff} is determined by M_s, H_k, the particle shape, and the volume fraction (μ^{p} and μ^{eff} will also depend on the particle conductivity and the particle size if eddy current losses are explicitly taken into account [19]). It is implicitly assumed in this work that the particles are all aligned in a way that their easy axes are parallel to each other and that the minor, major, and cylindrical axes, respectively, of the oblate ellipsoidal, prolate ellipsoidal, and cylindrical particles are coincident with their easy axes.

This paper is organized as follows: Section 2 provides details about the theoretical framework used here, Section 2.1 discusses the Bruggeman effective medium theory, and Section 2.2 describes how the FMR behavior of ellipsoidal and cylindrical particles can be included self-consistently within the Bruggeman EMT approach. Results are presented and discussed in Section 3. Finally, the conclusions of this work are summarized in Section 4.

---

[2]) In general, the permeability can be different along different hard axes. For instance, a disc (or thin film) with its easy axis parallel to the plane of the disc displays a high permeability (equal to the bulk value) along a direction normal to both the easy axis and the disc normal, while a very low permeability is displayed parallel to the disc normal. In the case of spheres and cylindrical rods with the easy axis along the rod axis (like the particles considered here), the permeabilities are equal along all the hard axes due to symmetry effects.

[3]) This is strictly true only in materials that show uniaxial crystal anisotropy (like Co). In the case of systems that display cubic crystal symmetry (like Fe), directions perpendicular to the easy axis can be other easy axes. Nevertheless, the permeability along any direction perpendicular to the saturation magnetization direction is still given by the formalism described here. We thus continue to use the nomenclature "hard" axis for directions orthogonal to the magnetization direction, even in the case of crystals that do not display uniaxial anisotropy.

[4]) In the case of a thin film (or disc) with its easy axis parallel to the plane of the film, "permeability" refers to the relative permeability along the direction normal to both the easy axis and the film normal.

2. Details of the Theoretical Framework

2.1 Bruggeman EMT

Many types of EMTs have been discussed in the literature [17, 18]; these theories attempted to determine the properties of the effective medium (like the effective permeability or the effective permittivity) in terms of the properties of the components for given component volume fractions. In the present work, we have used the Bruggeman EMT which is supported by experimental data [20].

For a two-component system with one component representing the ellipsoidal or cylindrical magnetic particles (with permeability μ^{p} and volume fraction c) and the other component representing the non-magnetic matrix (with permeability 1 and volume fraction $1-c$), the Bruggeman formalism leads to [21]

$$\frac{c(\mu^{\mathrm{p}}-\mu^{\mathrm{eff}})}{\mu^{\mathrm{eff}}+(\mu^{\mathrm{p}}-\mu^{\mathrm{eff}})\,N_k}+\frac{(1-c)\,(1-\mu^{\mathrm{eff}})}{\mu^{\mathrm{eff}}+(1-\mu^{\mathrm{eff}})\,N_k}=0\,. \tag{1}$$

Here, the particles are assumed to be aligned with their easy axes oriented along the z axis and N_k (with $k=x$ or y) is the shape factor (tabulated elsewhere [15][5]) of the particles along the direction of the rf magnetic field which is assumed to be transverse to the easy axis. We will consider this factor more detailed in Section 2.2; for spherical particles $N_{x,y}=1/3$.

2.2 FMR behavior of the composite

The solution of the Landau-Lifshitz equation [14, 15] yields the frequency dependent relative permeability tensor (in terms of M_{s}, H_k, and the shape factors of the particle). As mentioned earlier, we only focus on the low frequency permeability and the FMR frequency. The diagonal components of the low frequency relative permeability tensor for particles with their easy axis parallel to the z-axis are given by [14, 15]

$$\mu_{xx}=\frac{M_{\mathrm{s}}}{H_k+M_{\mathrm{s}}(A_x-A_z)}+1\,, \tag{2}$$

$$\mu_{yy}=\frac{M_{\mathrm{s}}}{H_k+M_{\mathrm{s}}(A_y-A_z)}+1\,, \tag{3}$$

$$\mu_{zz}=1\,, \tag{4}$$

μ_{xx} and μ_{yy} are the hard axes permeabilities, and μ_{zz} is the easy axis permeability. In the case of the particles considered here (ellipsoidal and cylindrical particles with the minor, major, and cylindrical axes of the oblate ellipsoids, prolate ellipsoids, and cylinders, respectively, coinciding with the easy axis), $\mu^{\mathrm{p}}\equiv\mu_{xx}=\mu_{yy}$ due to symmetry reasons. Within the present development, the demagnetizing factors $(A_x,A_y,A_z)\equiv\mathbf{A}$ include the effects due to volume fraction and are given by [22–24]

$$\mathbf{A}=\frac{\mu^{\mathrm{bulk}}-\mu^{\mathrm{eff}}}{\mu^{\mathrm{eff}}(\mu^{\mathrm{bulk}}-1)}\,\mathbf{N}\,, \tag{5}$$

[5]) See also Tables 1 and 2 for examples of demagnetizing factors. It should be noted that a zero demagnetizing shape factor along a particular direction implies that the demagnetizing field set up by an external field along that direction is zero.

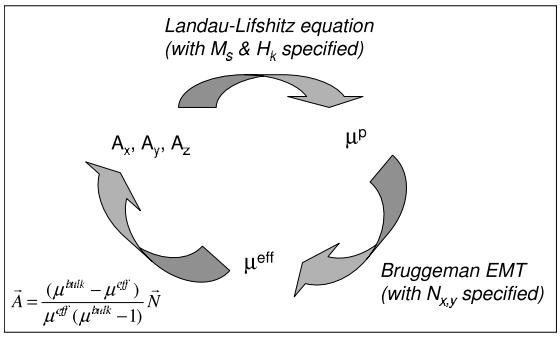

Fig. 1. Flowchart describing the process of self-consistently determining the particle and effective permeabilities at a non-zero particle volume fraction for non-spherical particles

where $\mathbf{N} \equiv (N_x, N_y, N_z)$ are the shape factors discussed above and $\mu^{\text{bulk}} = M_s/H_k + 1$ (equal to μ_{xx} and μ_{yy} with $\mathbf{A} = 0$; see below). In essence, $\mathbf{A}$ is the demagnetizing factor for a particle embedded in a medium with permeability μ^{eff} (as the Bruggeman EMT demands [17, 18]), while $\mathbf{N}$ is that for a particle embedded in a non-magnetic environment. It can be seen that $\mathbf{A}$ given by the above equation has the expected limiting behavior. For instance, at low volume fraction (isolated particle limit), $\mu^{\text{eff}} \approx 1$, implying $\mathbf{A} \approx \mathbf{N}$; at high volume fraction (bulk limit), $\mu^{\text{eff}} \approx \mu^{\text{bulk}}$, implying $\mathbf{A} \approx 0$, as one would expect for bulk materials.

When $A_x = A_y = A_z = A$, a condition satisfied by bulk materials and spherical particles embedded in any matrix (note that $A = 0$ and $A = 1/3$, respectively, in the case of bulk materials and in the case of an isolated spherical particle in a non-magnetic matrix), Eqs. (2) and (3) simplify to $\mu_{xx} = \mu_{yy} = M_s/H_k + 1$ (independent of A). Thus, the determination of μ^{eff} using Eq. (1) in the case of spherical particles requires only the knowledge of μ^p ($\equiv \mu_{xx} = \mu_{yy}$). In the case of non-spherical particles, however, the determination of μ^p requires the knowledge of $\mathbf{A}$, which in turn requires the knowledge of μ^{eff}. Thus, Eqs. (1)–(3), and (5) need to be solved self-consistently for a given magnetic particle volume fraction and particle shape. The solution process is heuristically depicted in Fig. 1 and needs to be performed iteratively[6]). The self-consistent solution (μ^p, μ^{eff}, and $\mathbf{A}$) is determined at zero frequency and the resulting $\mathbf{A}$ is used to calculate the FMR frequency of the composite using the well known Kittel equation [14, 25]

$$\omega_{\text{fmr}} = \mu_0 \gamma \sqrt{[H_k + (A_x - A_z)\, M_s]\, [H_k + (A_y - A_z)\, M_s]}, \tag{6}$$

where μ_0 is the permeability of free space and γ is the gyromagnetic ratio.

3. Results and Discussion

We now use the theory outlined above to investigate the relationship between the properties of the particles (M_s, H_k, shape, and volume fraction) and the magnetic properties of the composite (the low frequency effective permeability and the FMR frequency). Values of 2.4 T and 0.049 T were chosen for $\mu_0 M_s$ and $\mu_0 H_k$, respectively, correspond-

[6]) The self-consistent solution was obtained by discretizing the volume fraction axis in steps of 0.001 and determining μ^{eff} at a particular volume fraction step from μ^p, and $\mathbf{A}$ determined in the previous step; note that $\mathbf{A}(c = 0) = \mathbf{N}$.

Table 1

Analytical expressions for the low frequency relative permeability along the two hard axes and the FMR frequency for particles with different geometries; the easy axis is assumed to be parallel to the z-axis and $M_s \gg H_k$

shape	N_x	N_y	N_z	μ_{xx}	μ_{yy}	ω_{fmr}
bulk	0	0	0	$\frac{M_s}{H_k}+1$	$\frac{M_s}{H_k}+1$	$\mu_0\gamma H_k$
thin film[a])	1	0	0	~ 2	$\frac{M_s}{H_k}+1$	$\sim \mu_0\gamma\sqrt{M_s H_k}$
infinite rod[b])	0.5	0.5	0	~ 3	~ 3	$\sim \mu_0\gamma M_s/2$
sphere	1/3	1/3	1/3	$\frac{M_s}{H_k}+1$	$\frac{M_s}{H_k}+1$	$\mu_0\gamma H_k$

[a]) film normal parallel to x-axis
[b]) rod axis parallel to z-axis

ing to a bulk permeability ($= M_s/H_k + 1$) of 50. We first draw some general conclusions regarding the desired particle shape and the nature of the final packing geometry before we address the impact of the particle volume fraction.

The shape factors (N_x, N_y, N_z), the low frequency permeability (determined using Eqs. (2) and (3)), and the FMR frequency (determined using Eq. (6)) for some representative examples are listed in Tables 1 and 2. The FMR frequency is smallest for the bulk (and the sphere) configuration. The thin film configuration (with the easy axis along the surface of the film) shows the bulk low frequency permeability (albeit along only one direction) but a higher FMR frequency. Infinite or finite rods or cylinders (with the easy axis parallel to the cylinder axis) have even higher FMR frequencies than the thin film case but low permeabilities. Spheres have properties identical to the bulk. Rods or cylinders with the easy axis parallel to the radial direction are not considered here since the practical growth of such structures is not expected to be easy. From Tables 1 and 2 it is clear that nearly spherical particles (between spherical and rod like with an aspect ratio of 2) are desired, in order to achieve an optimal particle permeability *and* FMR frequency.

Table 2

Same as Table 1 with $\mu_0 M_s = 2.4$ T and $\mu_0 H_k = 0.049$ T (parameters chosen in this study); an additional entry for a finite rod with an aspect ratio of two has also been included ($f_{\mathrm{fmr}} = \omega_{\mathrm{fmr}}/2\pi$)

shape	N_x	N_y	N_z	μ_{xx}	μ_{yy}	f_{fmr} (GHz)
bulk	0	0	0	50	50	1.4
thin film[a])	1	0	0	2	50	9.7
infinite rod[b])	0.5	0.5	0	2.9	2.9	33.6
finite rod[c])	0.43	0.43	0.14	4.2	4.2	20.9
sphere	1/3	1/3	1/3	50	50	1.4

[a]) film normal parallel to x-axis
[b]) rod axis parallel to z-axis
[c]) rod axis parallel to z-axis; aspect ratio $= 2$

Another important factor to achieve a final geometric structure is the packing of the particles: assuming that the particles are all aligned so that their magnetization (easy) axes are parallel to each other, the particles can be packed in a way that either the bulk or the thin film final geometry limits are reached. Here, the "bulk limit" is defined as the situation when an appreciable magnetic field exists *only* in the interior of the composite system, i.e. the surfaces or boundaries of the composite system are located in regions of negligible magnetic field, thereby generating negligible demagnetizing fields in any direction. The "thin film limit" is defined as the situation when the thin film surfaces (but not the edges) are located in regions of appreciable magnetic field, thereby generating demagnetizing fields *only* along the film normal. The relationship between geometry and magnetic properties listed in Tables 1 and 2 indicates that the packing of (approximately spherical) particles achieving the thin film limit with the particle easy axes oriented along the film surface leads to a desired configuration.

It should be mentioned that the properties listed in Tables 1 and 2 for the rods and spheres hold only for isolated particles (N_x, N_y, N_z are the demagnetizing shape factors for *isolated* particles in a non-magnetic environment), corresponding to low magnetic particle volume fractions. An increase in the particle volume fraction implies that particles are no longer in a non-magnetic environment but embedded in an effective medium of permeability μ^{eff} which means the self-consistent procedure described in Section 2.2 should be adopted to determine μ^{eff} and $\mathbf{A}$ as a function of the volume fraction. It should be noted that the bulk and thin film limits are characterized by the demagnetizing factors (and by the low frequency permeability and f_{fmr}) listed in the first and third row of Tables 1 and 2, respectively, which must be reached again for $c \to 1$. Adopting the procedure outlined in Section 2.2 automatically ensures achieving the bulk limit ($\mathbf{A} \to 0$ as $c \to 1$). The thin film limit is achieved by using Eq. (5) for calculating A_y and A_z (both of which approach zero for $c \to 1$), and by requiring that $A_x = 1 - (A_y + A_z)$, such that the thin film demagnetizing factors are reached again for $c \to 1$. It should be noted that while the self-consistent procedure to determine μ^{eff} and f_{fmr} is not required in the case of spherical particles packed to achieve the bulk limit, this procedure is necessary in the case of spherical particles packed to achieve the thin film geometry.

Figures 2 and 3 show the low frequency effective permeability and the FMR frequency, respectively, as a function of the particle volume fraction for spherical and finite rod (aspect ratio 2) particles packed to achieve the bulk and the thin film limits. The values have been calculated using the procedure described in Section 2.2 with

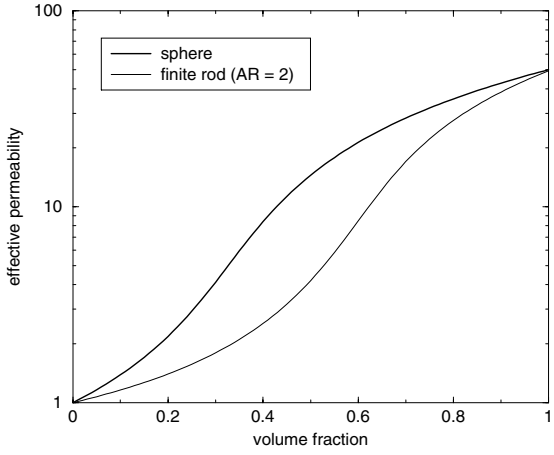

Fig. 2. Effective low frequency permeability, μ^{eff}, versus magnetic particle volume fraction for spherical and finite rod (aspect ratio of 2) particle composites determined by self-consistently solving Eqs. (1), (2), and (5); the packing type does not effect μ^{eff}

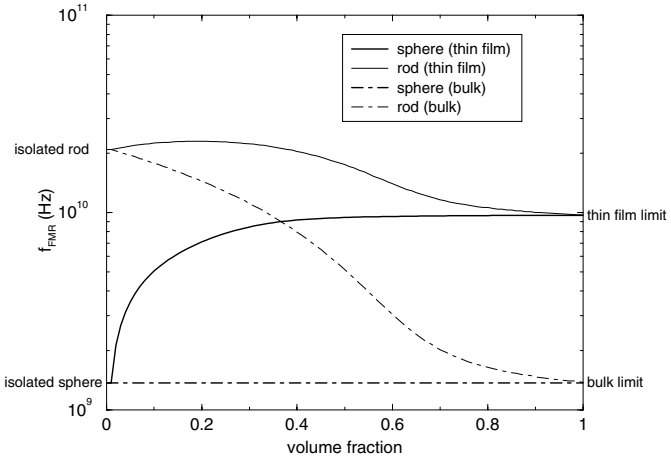

Fig. 3. FMR frequency, f_{fmr}, versus magnetic particle volume fraction for spherical and finite rod (aspect ratio of 2) particle composites determined by self-consistently solving Eqs. (1), (2), and (5). "Thin film" and "bulk" limit final geometry are shown

the modification identified above for the thin film limit. The packing limit affects the FMR frequency but not μ^{eff}, as the latter is calculated along the relevant hard axis (the one parallel to the film plane in the case of thin film packing) and the demagnetizing factor along this direction is the same for both packing types. As expected, μ^{eff} for the spherical particle composite is higher than for the finite rod composite. It should be noted that the maximum volume fractions achievable for spheres and cylinders with identical radii are 0.74 and 0.91, respectively. The FMR frequency for the bulk limit packing does not change with volume fraction for the spherical particle composite (as isolated spherical particles already have properties identical to that of the bulk), but decreases for the finite rod particle composite. For the thin film packing, f_{fmr} increases very fast for the spherical particle composite and reaches the saturation value of about 10 GHz at a volume fraction of ~ 0.4, whereas for the finite rod particle composite it decreases relatively slowly to the 10 GHz value. Assuming that achievable thin film packing densities of approximately spherical particles are in the 0.45–0.55 range, μ^{eff} values in the 3–18 range, and f_{fmr} values in the 18–10 GHz range can be expected (for the material parameters chosen here).

4. Summary

A phenomenological model of magnetic nanoparticle composites consisting of ideal lossless particles with identical properties embedded in a non-magnetic matrix has been developed. The input material parameters for this model include the saturation magnetization (M_{s}) and the crystal anisotropy field (H_k) of the particles. An attempt has been made to relate key magnetic properties like the low frequency effective permeability or the FMR frequency to the physical properties of the particles (such as shape, volume fraction, and packing type). For the material parameters of the particles chosen here ($\mu_0 M_{\mathrm{s}} = 2.4$ T and $\mu_0 H_k = 0.049$ T, resulting in a bulk permeability of 50), composites consisting of approximately spherical particles packed to achieve the thin film limit with

a volume fraction in the 0.45–0.55 range are expected to display low frequency effective permeability and FMR frequency values in the 3–18 and 18–10 GHz ranges, respectively.

Acknowledgements

We wish to acknowledge interactions and discussions with R. Stumpf and B. Engel (Physical Sciences Research Laboratory, Motorola, Inc.).

References

[1] M. SCHEFFLER, G. TRÖSTER, J. L. CONTRAS, J. HARTUNG, and M. MENARD, Microelectron. Int. **17/3**, 11 (2000).
[2] T. H. LEE, in: Proc. GAAS 99 Conf., Munich (Germany), Oct. 1999 (p. 8).
[3] Y. KOUTSOYANNOPOULOS, Y. PAPANANOS, S. BANTAS, and C. ALEMANNI, in: Proc. IEEE Int. Symp. Circuits and Systems, Geneva (Switzerland), May 2000 (p. II-160).
[4] K. D. CORNETT, in: Proc. Bipolar/BiCMOS Circuits and Technology Meeting, Piscataway (USA), 2000 (p. 187).
[5] T. J. KLEMMER, K. A. ELLIS, L. H. CHEN, R. B. VAN DOVER, and S. JIN, J. Appl. Phys. **87**, 830 (2000).
[6] S. JIN, W. ZHU, R. B. VAN DOVER, T. H. TIEFEL, V. KORENIVSKI, and L. H. CHEN, Appl. Phys. Lett. **70**, 3161 (1997).
[7] M. YAMAGUCHI, K. SUEZAWA, K. I. ARAI, Y. TAKAHASHI, S. KIKUCHI, Y. SHIMADA, W. D. LI, S. TANABE, and K. ITO, J. Appl. Phys. **85**, 7919 (1999).
[8] J. HUIJBREGTSE, F. ROOZEBOOM, J. SIETSMA, J. DONKERS, T. KUIPER, and E. VAN DE RIET, J. Appl. Phys. **83**, 1569 (1998).
[9] E. VAN DE RIET and F. ROOZEBOOM, J. Appl. Phys. **81**, 350 (1997).
[10] S. SUN and D. WELLER, J. Magn. Soc. Jpn. **25**, 1434 (2001).
[11] C. DE JULIAN FERNANDEZ, C. SANGRERORIO, G. MATTEI, C. MAURIZIO, G. BATTAGLIN, F. GONELLA, A. LASCIALFARI, S. LO RUSSO, D. GATTESCHI, P. MAZZOLDI, J. M. GONZALEZ, and F. D'ACAPITO, Nucl. Instrum. Methods Phys. Res. B **175–177**, 479 (2001).
[12] U. WEIDWALD, M. SPASOVA, M. FARLE, M. HILGENDORFF, and M. GIERSIG, J. Vac. Sci. Technol. A **19**, 1773 (2001).
[13] M. RESPAUD, M. GOIRAN, J. M. BROTO, F. H. YANG, T. OULD ELY, C. AMIENS, and B. CHAUDRET, Phys. Rev. B **59**, R3934 (1999).
[14] D. M. POZAR (Ed.), Microwave Engineering, Wiley, New York 1998.
[15] R. C. O'HANDLEY (Ed.), Modern Magnetic Materials: Principles and Applications, Wiley, New York 1999.
[16] D. A. G. BRUGGEMAN, Ann. Phys. (Germany) **24**, 636 (1935).
[17] K. K. KARKKAINEN, A. H. SIHVOLA, and K. I. NIKOSKINEN, IEEE Trans. Geoscience Remote Sensing **38**, 1303 (2000).
[18] D. E. ASPNES, Am. J. Phys. **50**, 704 (1982).
[19] R. RAMPRASAD, P. ZURCHER, M. PETRAS, M. MILLER, and P. RENAUD, to be published.
[20] J. H. PATERSON, R. DEVINE, and A. D. R. PHELPS, J. Magn. Magn. Mater. **196–197**, 394 (1999).
[21] M. LE FLOC'H, A. CHEVALIER, and J. L. MATTEI, J. Phys. IV (France) **8**, 355 (1998).
[22] J. A. STRATTON (Ed.), Electromagnetic Theory, McGraw-Hill Publ. Co., New York (1941).
[23] J. L. MATTEI and M. LE FLOC'H, J. Magn. Magn. Mater. **215/216**, 589 (2000).
[24] A. CHEVALIER, J. L. MATTEI, and M. LE FLOC'H, J. Magn. Magn. Mater. **215/216**, 66 (2000).
[25] CH. KITTEL (Ed.), Introduction to Solid State Physics, Wiley, New York 1995.